Journal of Physics B: Atomic, Molecular and Optical Physics

PAPER

Multiplet exchange Auger transitions following resonant Auger decays in Ne 1s photoexcitation

To cite this article: Yusuke Tamenori and Isao H Suzuki 2014 *J. Phys. B: At. Mol. Opt. Phys.* **47** 145001

IOP Publishing Journal of Physics B: Atomic, Molecular and Optical Physics
J. Phys. B: At. Mol. Opt. Phys. **47** (2014) 145001 (9pp) doi:10.1088/0953-4075/47/14/145001

Multiplet exchange Auger transitions following resonant Auger decays in Ne 1s photoexcitation

Yusuke Tamenori[1] **and Isao H Suzuki**[2]

[1] Synchrotron Radiation Research Institute/SPring-8, 1-1-1 Kouto, Sayo, 679-5198, Japan
[2] Institute of Materials Structure Science, High Energy Accelerator Research Organization (KEK), 1-1 Oho, Tsukuba 305-0801, Japan, and Advanced Institute of Industrial Science and Technology (AIST), 1-1-1 Umezono, Tsukuba 305-8568, Japan

E-mail: tamenori@spring8.or.jp

Received 16 February 2014, revised 15 May 2014
Accepted for publication 3 June 2014
Published 4 July 2014

Abstract

Secondary electron emission with very low kinetic energy (KE) has been measured in the Ne 1s photoexcitation region. A new decay channel for Auger transitions following Ne 1s to 3p excitation has been identified using a two-dimensional mapping technique, in which slow Auger electron signals are displayed as functions of electron kinetic energy and photon energy. Electrons with about 0.68 eV KEs have been ascribed to multiplet exchange Auger electrons from the $2p^{-2}(^1S)3d$ state. This state is formed through the resonant Auger transition from the $1s^{-1}3p$ state, in which the excited 3p electron changes its azimuthal quantum number. Another cascade Auger decay of multiplet exchanging was found as electron emission of about 2.0 eV KEs; $2p^{-2}(^1S)4p \rightarrow 2p^{-2}(^3P) + e^-$. Several cascade decays were found to occur via the photoexcitation into $1s^{-1}4p$ and $1s^{-1}5p$ states.

Keywords: multiplet-changing, Ne 1s photoexcitation, cascade Auger, low energy electrons

(Some figures may appear in colour only in the online journal)

1. Introduction

Electron spectroscopy for photoelectrons and Auger electrons of atoms and molecules has undergone significant progress in recent decades. This progress stems from improvements in experimental apparatuses and techniques, which are mainly related to advances in soft x-ray synchrotron radiation with tunable energy and polarization and in high-luminosity electron spectrometers. This improvement enables us to perform finer studies of rare gas atoms, as well as pursue highly correlated targets such as ionic and open-shell species. Resonant Auger electron emission processes have been investigated for a number of atoms and molecules by many research groups; in particular, resonant photoexcitation of Ne 1s electrons was studied as a typical showcase of rare gas atoms [1–6]. Lifetime broadening, interference phenomena, and Auger Raman effects related to the resonant Auger transitions have been clarified using narrow band-pass photon beam and high-resolution electron spectrometers for rare gas atoms [1–10]. A resonant Auger transition of the spectator type, in which the final state is expressed with a state of two orbital holes and one excited electron, usually dominates a participator one, corresponding to a state of conventional photoelectron signals. The spectator electron remains in the excited orbital at the first step, but a substantial portion of the decay distributes to a shaken-up process; the principal quantum number n is changed to $n+1$ in many instances, but keeps the same azimuthal quantum number. This shake-up phenomenon is interpreted with a theoretical model of shake modified resonant Auger effect [7, 11, 12], and this model can be used to interpret shake-down transitions; the original n orbital electron moves to $n-1$ orbital. A few examples of change in the azimuthal quantum number were reported to occur with appreciable yields for the photoexcitation of Kr 3d electrons and Xe 4d electrons into np orbitals [7, 11]. These findings were inferred to originate from interchannel coupling due to interaction of the same total angular momentum states between spectator decays and participator ones.

When resonant Auger final states still hold some energy higher than the threshold energy of the doubly charged ion, secondary electrons are usually emitted as cascade electrons. These processes were measured for rare gas atoms using resonant inner-shell photoexcitation and valence shake-up photoionization [13–20]. Because the inner valence s orbital has higher binding energy than the outer valence p orbital, the states with one inner valence hole and one outer valence hole are positioned higher than the first double ionization threshold, which is two outer valence holes states (np^{-2}). Several measurements on cascade Auger decays of intervalence changing from Ne $1s^{-1}np$ states were reported [14–19], in which the assignments were supported by theoretical calculations using the multiconfiguration Dirac–Fock method. The $2p^{-2}$ configuration of Ne corresponds to three multiplets of ^3P, ^1D, and ^1S in the L–S coupling scheme and the related energy positions are 62.53 eV for the $^3P_2$ state, 65.73 eV for the $^1D_2$ state, and 69.44 eV for the $^1S_0$ state [21]. This situation means that some Rydberg states of the $2p^{-2}$ np type can occasionally emit a second electron; e.g., the $^1S_0$ np state being higher than the ^3P state turns into a doubly charged ion of ^3P and a secondary electron with very low kinetic energy (KE) [15, 17, 21]. When the quantum number is high, a number of emission channels are expected to exist. De Fanis *et al* precisely studied the cascade Auger electron emission using an elaborate technique for production of $2p^{-2}$ np states, in which slow photoelectrons are recaptured in the ion core and many $2p^{-2}$ np states with high n values are formed at photoexcitation near the 1s ionization threshold [15, 17]. Becker *et al* investigated double ionization phenomena through valence shake-up photoionization using monochromatic vacuum ultraviolet radiation in combination with calculations by the many-body perturbation theory [20]. Threshold photoelectron spectra were measured in the region of the double ionization energy of the $2p^{-2}$ configuration, which discovered several ionic excited states of $2p^{-2}nl$ configurations [22]. These studies gave us a variety of information on the $2p^{-2}nl$ states because the cascade processes depend on different mechanisms being related to intermediate states, selection rules, and production yields.

A graphical technique often provides productive information on the analysis of experimental data and prevents us from incorrectly interpreting physical phenomena. The dependence of signals of interest on excitation energy, auxiliary product yields, and detection direction provides meaningful data on the mechanisms of the dynamical processes of atoms and molecules in excited or ionic states. Several examples of atoms and molecules in core-hole states were reported using two-dimensional (2D) mapping of exciting photon energy and electron KE [4, 23–28]. These reports clarified complicated phenomena, providing important results about the dynamical processes of atoms and molecules.

In the present study, secondary electrons with low KE following the Ne 1s resonant Auger decays are measured using a hemispherical electron spectrometer. Using the 2D mapping technique, electrons with about 0.65 and 2.0 eV KEs are ascribed to multiplet exchange Auger electrons. A new decay channel is identified in the cascade Auger decay from the ^1S 3d state via 1s to 3p photoexcitation.

2. Experimental

Measurements were performed on the c branch of the soft x-ray photochemistry beamline BL27SU at the SPring-8 facility [29]. This facility was operated with a ring current of 100 mA under the top-up mode. This beamline provided linearly polarized monochromatic light ranging from 0.17 to 2.8 keV [30]; the degree of polarization was higher than 0.98 at the tuning of the first-order radiation with the horizontal polarization [31]. The energy calibration of the monochromator was performed using the Ne 1s photoelectrons and the Ne 1s photoabsorption spectrum [32, 33]. The photon bandwidth employed was about 0.15 eV in most instances. The intensity of the monochromatized incident photon beam during the measurement was monitored by collecting the drain current of the post-focusing mirror in the beamline.

The electron spectrometer used consisted of a hemispherical electron spectrometer (Gammadata Scienta, SES-2002) fitted to a gas cell (GC-50) by way of a multi-element lens in a differentially pumped chamber [8]. Sample gas of Ne was supplied into the gas cell and the gas density observed was about 2×10^{-4} Pa in the chamber during the measurements. The direction of the electric vector can be switched to be either parallel or perpendicular to the axis of the electrostatic lens of the analyzer by varying the gap of the undulator, and, in this way, we can perform the angle-resolved electron spectroscopy with one electron energy spectrometer fixed to the horizontal direction [8]. The pass energy of the spectrometer was fixed at 2 eV to measure cascade Auger electrons and fixed at 100 eV for resonant Auger electrons. The spectrometer parameters were set such that the energy width of the electrons detected was 0.05 eV for 2 eV pass energy and 0.15 eV for 100 eV pass energy. The electron energy was calibrated using Ne 2p photoelectrons at the 2 eV pass energy and using the peak energies for the KLL-Auger decay from the Ne 1s-shell hole states at the 100 eV pass energy [34]. Collection efficiency was varied for suppression of backgrounds beacuse low-energy electrons mainly came from scattering with the surface of the electrodes. Thus, the discussion on quantitative electron yields for energies lower than 5 eV is not meaningful in the present study.

Total ion yield (TIY) spectra were measured at the midpoint between the post-focusing mirror and the electron spectrometer using a microchannel plate assembly with focusing electrodes.

3. Results and discussion

3.1. Electron emission at first step

At first, resonant Auger electron spectra at several photon energies near the Ne 1s ionization energy have been measured to obtain a clue of the resonant Auger final states, which are

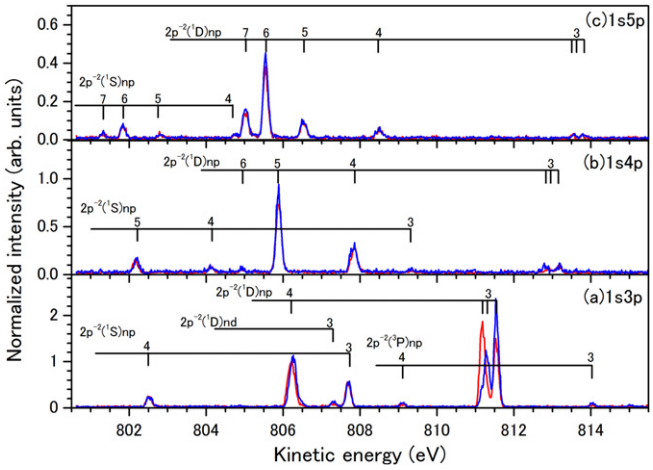

Figure 1. Resonant Auger electron spectra from 801–815 eV at the photon energies of 867.1 eV ($1s^{-1}3p$), 868.7 eV ($1s^{-1}4p$), and 869.3 eV ($1s^{-1}5p$) from the bottom to the top; (a), (b), and (c). Red curves denote the spectra at the parallel polarization of the incident photon beam and blue curves denote those at the perpendicular polarization.

Table 1. Relative yields of resonant Auger final states related to shake effect.

Initial excited orbital	Quantum number of the final orbital 3	4	5	6	7	Remark
3p	0.69	0.31	<0.01	<0.01	<0.01	Present
	0.68	0.32	<0.01	<0.01	<0.01	[3]
4p	0.08	0.26	0.64	0.02	<0.01	Present
	0.08	0.25	0.64	0.03	<0.01	[3]
5p	0.04	0.08	0.14	0.52	0.22	Present
	<0.01	0.07	0.13	0.53	0.23	[3]

presumed to become initial states of the second step process. Figure 1 shows resonant Auger electron spectra measured at three photon energies corresponding to excitation into 3p (867.1 eV), 4p (868.7 eV), and 5p (869.3 eV) states, in figures 1(a)–(c), respectively. The blue curves display the spectra at the parallel photon polarization and the red curves display those at the perpendicular polarization. The resonant Auger spectra and their related phenomena have been reported by several researchers [1–6, 8] and only important points are indicated here. In figure 1(a), the peaks with the highest signal intensity occur near the electron KE of 811.3 eV. This excitation-decay process is expressed in the following manner [1–3]:

$$\mathrm{Ne} + \mathrm{h}\nu \rightarrow \mathrm{Ne}^{*}\left(1s^{-1}3p\right) \rightarrow \mathrm{Ne}^{+}\left(2p^{-2}\left(:^{1}\mathrm{D}\right)3p\right) + e^{-}. \quad (1)$$

The configuration of $2p^{-2}(:^{1}D)3p$ forms several states of multiplets (^{2}P, ^{2}D, and ^{2}F), whose binding energies were reported at 55.83 eV for $^{2}P_{3/2}$, 55.95 eV for $^{2}D_{3/2}$, and 55.58 for $^{2}F_{5/2}$, respectively [3, 35]. The measured peaks indicate considerable angular discrimination for these states. The anisotropy parameters (β) were estimated for three transitions as follows: 0.32 for ^{2}F, 0.81 for ^{2}P, and −0.85 for ^{2}D. These values are not so different from the data in the literature (0.27 for ^{2}F, 0.98 for ^{2}P, and −0.95 for ^{2}D) [8]. Other peaks, to which some labels are added in figure 1(a), consist of one excited electron at the 3p or 4p orbital and of two 2p holes (^{1}S, ^{1}D, and ^{3}P). For example, peaks around 802.5, 806.2, 807.7, and 809.1 eV correspond to final states of $2p^{-2}(^{1}S)4p$, $(^{1}D)4p$, $(^{1}S)3p$, and $(^{3}P)4p$, respectively.

The Auger shake-up transitions of 3p excited electrons to the 4p orbital occur often [1–3]. In figure 1(b), many peak structures occur and intensities of shake-up peaks increase to some extent at the 4p photoexcitation level. Further, a shake-down transition is found to occur from the peaks with low intensity around the electron energy of 813 eV. In this instance, the 4p excited electron moves to the 3p orbital during the Auger decay. The 5p excitation [figure 1(c)] yields a significant increase of intensity for the states with the 6p excited electron. The shake effect for the $^{1}D_{2}$ core-hole states was determined at the three photon energies and listed in table 1. The results are in agreement with the data in a previous study [3]. Anisotropic effects are not seen to occur significantly in the 4p and 5p excitation levels.

It is important to examine resonant Auger electron spectra as a function of incident photon energy. Figure 2 shows the 2D map of the Auger decays in the parallel direction, which displays the electron signals as functions of the incident photon energy (865.5 ~ 871 eV) and the Auger electron energy (800 ~ 815 eV). These figures include the TIY spectrum at the right end, where the bars with hatching denote the 1s ionization threshold and labels added to peaks indicate excited orbitals. The islands around 806.2, 807.5, and 811 eV at the photon energy of 867 eV indicate transitions into to the final states of $2p^{-2}(^{1}D)4p$, $(^{1}S)3p$, and $(^{1}D)3p$, respectively. The photoexcitation to higher Rydberg orbitals provides similar characteristics of signal profiles to that of the 3p orbital. Diagonal lines in the 2D map show KEs of relaxation into some $2p^{-2}np$ final states. These excitation-decay processes display elliptical island structures along the diagonal direction in the 2D map. Shake phenomena, as well as complete spectator decays, occur often. In other words, these island structures of the diagonal lines have been yielded by a combination between the short lifetime (energy-broadening) and shake effects [6]. Above the ionization threshold, the normal Auger decay to the ^{1}D state (around 804.5 eV) occurs with a high yield, which exhibits a thick-vertical island with a bent structure near the ionization threshold in the 2D map. This bent structure is caused by an energy shift and distortion of the Auger peak, originating from a post-collision interaction with a slow 1s photoelectron [4–6]. A similar thick-vertical island is seen with low intensities around 801 eV, which corresponds to the Auger decay to the ^{1}S state.

Let us note an interesting point here. The small peak at the photon energy of 867.1 eV in figure 1(a) has appeared clearly at 807.3 eV, near where the high yield peak of the decay into the ^{1}S 3p state occurs. Although the authors did not give a clear assignment [3], the previous study on resonant Auger decays showed a small structure around 807.3 eV at the photon energy of 867.1 eV. Previous studies of other

Table 2. Assignments and physical quantities related to the cascade Auger decay: electron KE, initial and final states, term value, quantum number, and quantum defect. Unit of energy is of eV.

				Present study				Becker *et al* [20]				De Fanis *et al* [17]			
Excited orbital	Initial state		Final state	Kinetic energy	term value	n	δ	Kinetic energy	term value	n	δ	Kinetic energy	term value	n	δ
3p	^{1}S 4d	^{2}D	^{1}D					0.2	3.51	4	0.06*				
	^{1}S 5s	^{2}S	^{1}D					0.25	3.46	5	1.03*				
	^{1}D 5p	^{2}D	^{3}P					0.35	2.85	5	0.63*				
	^{1}D 5p	^{2}P	^{3}P					0.40	2.80	5	0.59*				
	^{1}S 3d	^{2}D	^{3}P$_{0,1}$	0.60	6.23	3	0.05	0.60	6.31	3	0.06*				
	^{1}S 3d	^{2}D	^{3}P$_{0,1}$	0.65	6.18	3	0.03								
	^{1}S 3d	^{2}D	^{3}P$_2$	0.68	6.23	3	0.05	0.70	6.21	3	0.04*				
	^{1}S 3d	^{2}D	^{3}P$_2$	0.72	6.19	3	0.04								
	^{1}S 5p	^{2}P	^{1}D					0.8	2.91	5	0.68*				
	^{1}D 5d	^{2}P	^{3}P					0.95	2.25	5	0.09				
	^{1}D 6p	^{2}D	^{3}P					1.20	2.00	6	0.79*				
	^{1}D 6p	^{2}P	^{3}P					1.24	1.96	6	0.74*				
	^{1}D 6d	^{2}P	^{3}P					1.65	1.55	6	0.08				
	^{1}D 7d	^{2}P	^{3}P					2.05	1.15	7	0.13				
	^{1}S 4p	^{2}P	^{3}P$_0$	1.97	4.83	4	0.64								
	^{1}S 4p	^{2}P	^{3}P$_1$	2.01	4.82	4	0.64	2.08	4.83	4	0.64				
	^{1}S 4p	^{2}P	^{3}P$_2$	2.08	4.83	4	0.64								
	^{1}S 5p	^{2}P	^{3}P					4.02	2.89	5	0.66*				
4p	^{1}D 5p	^{2}F	^{3}P$_0$	0.22	2.87	5	0.65					0.212	2.878	5	0.651
	^{1}D 5p	^{2}D	^{3}P$_0$	0.25	2.87	5	0.65					0.260	2.830	5	0.615
	^{1}D 5p	^{2}F,	^{3}P$_1$									0.246	2.878	5	0.651
	^{1}D 5p	^{2}D	^{3}P$_1$	0.29	2.83	5	0.62					0.294	2.830	5	0.615
	^{1}D 5p	^{2}F	^{3}P$_2$	0.32	2.88	5	0.66					0.326	2.878	5	0.651
	^{1}D 5p	^{2}D	^{3}P$_2$	0.37	2.83	5	0.62					0.374	2.830	5	0.615
	^{1}S 5p	^{2}P	^{1}D	0.84	2.87	5	0.65					0.852	2.856	5	0.635
	^{1}D 6p	^{2}F	^{3}P$_0$	1.21	1.91	6	0.67					1.191	1.899	6	0.647
	^{1}D 6p	^{2}D	^{3}P$_0$									1.216	1.874	6	0.611
	^{1}D 6p	^{2}D	^{3}P$_1$	1.24	1.88	6	0.63					1.250	1.874	6	0.611
	^{1}D 6p	^{2}F	^{3}P$_2$	1.30	1.90	6	0.65					1.305	1.899	6	0.647
	^{1}D 6p	^{2}D	^{3}P$_2$	1.32	1.88	6	0.63					1.330	1.874	6	0.611
	^{1}S 6p	^{2}P	^{1}D	1.83	1.88	6	0.62								
	^{1}S 4p	^{2}P	^{3}P$_0$	1.97	4.83	4	0.64								
	^{1}S 4p	^{2}P	^{3}P$_1$	2.01	4.82	4	0.64								
	^{1}S 4p	^{2}P	^{3}P$_2$	2.08	4.83	4	0.64								
	^{1}S 5p	^{2}P	^{3}P$_0$	3.95	2.85	5	0.63					3.943	2.855	5	0.634
	^{1}S 5p	^{2}P	^{3}P$_1$	3.97	2.86	5	0.64					3.977	2.855	5	0.634
	^{1}S 5p	^{2}P	^{3}P$_2$	4.06	2.85	5	0.63					4.057	2.855	5	0.634
5p	^{1}D 5p	^{2}F	^{3}P$_0$	0.22	2.87	5	0.65					0.212	2.878	5	0.651
	^{1}D 5p	^{2}D	^{3}P$_0$	0.25	2.87	5	0.65					0.260	2.830	5	0.615
	^{1}D 5p	^{2}F	^{3}P$_1$									0.246	2.878	5	0.651
	^{1}D 5p	^{2}D	^{3}P$_1$	0.29	2.83	5	0.62					0.294	2.830	5	0.615

Table 2. (Continued.)

				Present study				Becker *et al* [20]				De Fanis *et al* [17]			
Excited orbital	Initial state		Final state	Kinetic energy	term value	n	δ	Kinetic energy	term value	n	δ	Kinetic energy	term value	n	δ
	^{1}D 5p	^{2}F	$^3P_2$	0.32	2.88	5	0.66					0.326	2.878	5	0.651
	^{1}D 5p	^{2}D	$^3P_2$	0.37	2.83	5	0.62					0.374	2.830	5	0.615
	^{1}S 5p	^{2}P	^{1}D	0.84	2.87	5	0.65					0.852	2.856	5	0.635
	^{1}D 6p	^{2}F	$^3P_0$	1.19	1.90	6	0.65					1.191	1.899	6	0.647
	^{1}D 6p	^{2}D	$^3P_0$	1.21	1.91	6	0.67					1.216	1.874	6	0.611
	^{1}D 6p	^{2}F	$^3P_1$									1.225	1.899	6	0.647
	^{1}D 6p	^{2}D	$^3P_1$	1.24	1.88	6	0.63					1.250	1.874	6	0.611
	^{1}D 6p	^{2}F	$^3P_2$	1.30	1.90	6	0.65					1.305	1.899	6	0.647
	^{1}D 6p	^{2}D	$^3P_2$	1.32	1.88	6	0.63					1.330	1.874	6	0.611
	^{1}D 7p	^{2}F	$^3P_0$	1.75	1.34	7	0.63					1.742	1.348	7	0.646
	^{1}D 7p	^{2}D	$^3P_0$	1.77	1.35	7	0.66					1.757	1.333	7	0.610
	^{1}D 7p	^{2}F	$^3P_1$									1.776	1.348	7	0.646
	^{1}D 7p	^{2}D	$^3P_1$	1.78	1.34	7	0.64					1.791	1.333	7	0.610
	^{1}D 7p	^{2}F	$^3P_2$	1.85	1.35	7	0.66					1.856	1.348	7	0.646
	^{1}D 7p	^{2}D	$^3P_2$	1.86	1.34	7	0.64					1.871	1.333	7	0.610
	^{1}D 8p	^{2}F, ^{2}D	^{3}P	2.09	1.00	8	0.62					2.085	1.006	8	0.645
	^{1}D 8p	^{2}F, ^{2}D	^{3}P	2.20	1.00	8	0.64					2.199	1.006	8	0.645
	^{1}S 7p	^{2}P	^{1}D	2.37	1.34	7	0.63					2.367	1.314	7	0.630
	^{1}S 5p	^{2}P	$^3P_0$	3.97	2.86	5	0.64					3.943	2.855	5	0.634
	^{1}S 5p	^{2}P	$^3P_1$									3.977	2.855	5	0.634
	^{1}S 5p	^{2}P	$^3P_2$	4.06	2.85	5	0.63					4.057	2.855	5	0.634

*Values like quantum defects were estimated from their figures in the present study.

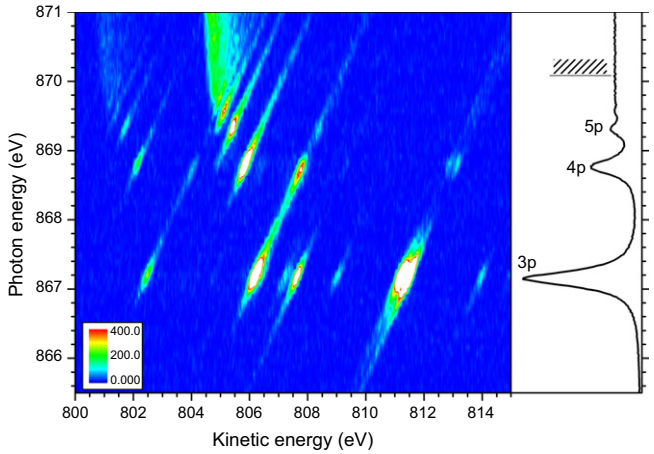

Figure 2. 2D map of photon energy (865.5–871 eV) and of resonant Auger electrons energy (800–815 eV) in the direction of the parallel polarization. At the right end, the TIY spectrum is exhibited with labels for excited Rydberg orbitals. The bar with hatching denotes the 1s ionization threshold.

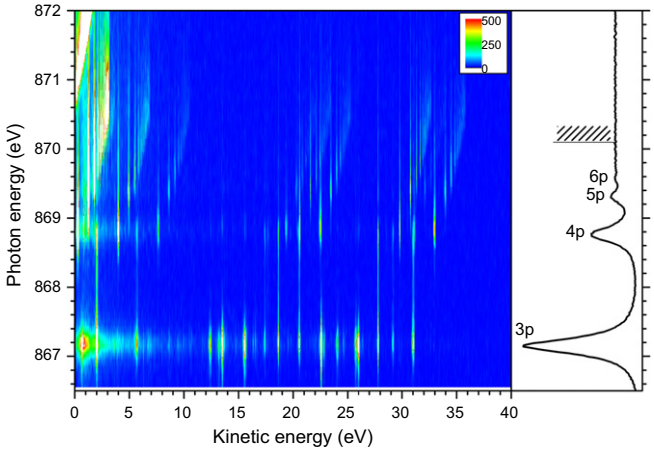

Figure 3. 2D map of photon energy (866.5–872 eV) and of secondary electron energy (0.1–40 eV) at the parallel polarization. At the right end, the TIY spectrum is exhibited with labels for excited Rydberg orbitals. The bar with hatching denotes the 1s ionization threshold.

rare gas atoms indicated that the azimuthal quantum number occasionally changes during resonant Auger transitions with low yields [7, 11]. This small peak in figure 1 is presumed to come from the decay of the azimuthal quantum number change in the excited 3p electron (spectator electron) to the 3d orbital and corresponds to the final state of ^{1}D 3d. Based on the database in NIST [21], energy levels corresponding to the ^{1}D 3d configuration are positioned at approximately 59.6 eV. The decays to these energy levels yield a peak around 807.5 eV.

3.2. Electron emission at second step

Figure 3 shows a 2D map of electron signals as functions of the photon energy (866.5–872 eV) and of the KE of the second step electron (0.1–40 eV), together with the TIY spectrum at the right end. This measurement was carried out in the direction of the parallel polarization. It is found that a number of thin-vertical island structures are located below the 1s ionization threshold. In contrast to the resonant Auger decay processes indicated in figure 2, these secondary electrons exhibit only vertical lines because the KE of the secondary electron is independent of the excitation photon energy. These structures above the electron energy of about 7 eV originate from the Auger cascade decays of configuration changing type (intervalence changing) [14, 16, 18]. For example, at the photon energy of 867.1 eV, the islands located at 13.5, 22.6, and 27.8 eV correspond to the following schemes, respectively:

$$\mathrm{Ne}^{+}\left(2\mathrm{s}^{-2}\left(:^{1}\mathrm{S}\right)3\mathrm{p}\right)+\mathrm{e}^{-}\rightarrow\mathrm{Ne}^{2+}\left(2\mathrm{s}^{-1}2\mathrm{p}^{-1}:^{1}\mathrm{P}\right)+2\mathrm{e}^{-}\left(\mathrm{KE}=13.5\mathrm{eV}\right)\quad(2)$$

$$\mathrm{Ne}^{+}\left(2\mathrm{s}^{-1}2\mathrm{p}^{-1}\left(:^{1}\mathrm{P}\right)3\mathrm{p}\right)+\mathrm{e}^{-}\rightarrow\mathrm{Ne}^{2+}\left(2\mathrm{p}^{-2}:\,^{1}\mathrm{D}\right)+2\mathrm{e}^{-}\left(\mathrm{KE}=22.6\mathrm{eV}\right)\quad(3a)$$

$$\mathrm{Ne}^{+}\left(2\mathrm{s}^{-1}2\mathrm{p}^{-1}\left(:^{1}\mathrm{P}\right)4\mathrm{p}\right)+\mathrm{e}^{-}\rightarrow\mathrm{Ne}^{2+}\left(2\mathrm{p}^{-2}:\,^{3}\mathrm{P}\right)+2\mathrm{e}^{-}\left(\mathrm{KE}=27.8\mathrm{eV}\right)\quad(3b)$$

The present results here mentioned are in agreement with previous studies that have described the initial states and final states related to these Auger cascade decays in detail [16, 18]. Below an electron energy of about 7 eV, electron signals of islands come from the Auger cascade decays of multiplet exchange type [17], as follows:

$$\mathrm{Ne}^{*}\left(1\mathrm{s}^{-1}\mathrm{np}\right)\rightarrow\mathrm{Ne}^{+}\left(2\mathrm{p}^{-2}\left(:^{1}\mathrm{S}\right)\mathrm{np}\right)+\mathrm{e}\rightarrow\mathrm{Ne}^{2+}\left(2\mathrm{p}^{-2}:\,^{1}\mathrm{D}\right)+2\mathrm{e}^{-}\quad(4)$$

Here, let us examine the low KE region of the 2D map more closely. Figure 4 displays the 2D maps with an enlarged scale in the electron energy of 0.1–7.5 eV. The measured results at the parallel polarization and perpendicular polarization are exhibited in figures (a) and (b), respectively. It is found that a diagonal band with very high intensity exists at a low KE region above the ionization threshold in figure 4(a). This band seems to become relatively narrow near the ionization threshold and this feature comes from the distortion of the 1s photoelectron peak from the post-collision interaction. The 2D map in figure 4(b) does not show this diagonal band owing to asymmetric emission of the 1s photoelectron. The series of the thin-vertical lines indicates convergence to some energy, which is presumed to correspond to the energy difference between the multiplets of the $2p^{-2}$ configuration, 3.20, 3.71, and 6.91 eV. Both 2D maps distinctly display the convergence at 3.20 eV and the map at the perpendicular polarization shows the convergence at 6.91 eV. However, the limit at 3.71 eV is not clearly seen because of the low yield of the ^{1}S *n*p series.

The electron emission at the second step from high Rydberg states, $2p^{-2}np$ ($n>4$), was investigated very precisely in combination with the sophisticated experimental work with multiconfiguration Dirac–Fock calculations [17]. For lower Rydberg states, the measurement was carried out for Auger cascade processes through valence double

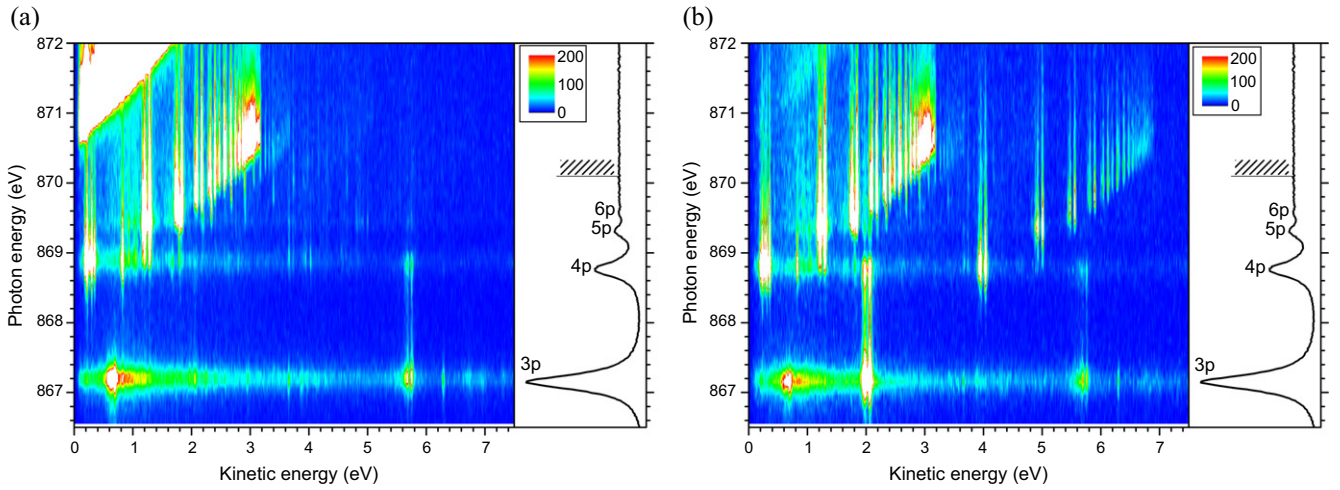

Figure 4. 2D maps of photon energy (866.5–872 eV) and of secondary electron energy (0.1–7.5 eV): (a) for the parallel polarization and (b) for the perpendicular polarization. At the right end, the TIY spectrum is exhibited with labels for excited Rydberg orbitals. The bar with hatching denotes the 1s ionization threshold.

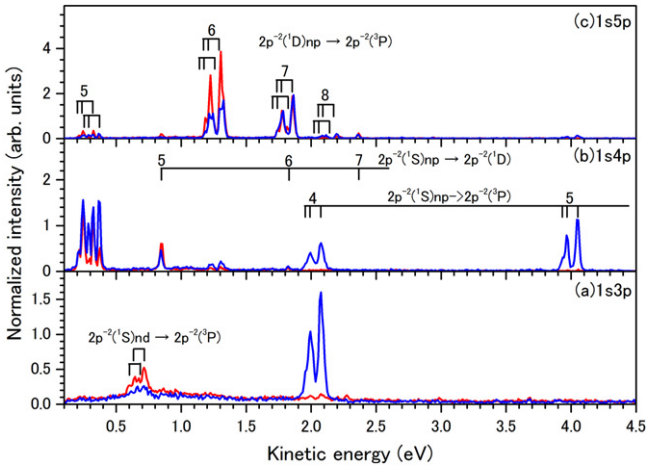

Figure 5. Secondary electron spectra from 0.1–4.5 eV at 867.1 eV ($1s^{-1}3p$), 868.7 eV ($1s^{-1}4p$), and 869.3 eV ($1s^{-1}5p$) recorded at 0° (red curve) and 90° (blue curve) relative to the polarization vector of incident photon beam, from the bottom to the top: (a), (b), and (c). Bars denote peaks or structures with intensity increase and some labels indicate their assignments.

photoexcitation, in other words, valence shake-up photoionization that yielded valence photoelectron satellites [20]. This measurement provided the assignments of the intermediate states (initial states at the second step) in the electron KEs of 0.15–6 eV.

At excitation to the $1s^{-1}3p$ state, islands are found around 0.7 and 2 eV, as shown in figure 4. For precise analysis of electron signals, the intensity distribution along the horizontal direction of the 2D maps (spectrum of electron signals) has been derived from figure 4. Figure 5(a) displays the spectrum of secondary electrons of 0.1–4.5 eV at the photon energy of 867.1 eV. Peaks with high intensity near 2 eV are assigned to the decay of the multiplet exchange from the ^{1}S 4p state produced via the shake-up Auger transition. This decay is expressed as follows:

$$\mathrm{Ne}^{*}\left(1s^{-1}3p\right) \rightarrow \mathrm{Ne}^{+}\left(2p^{-2}\left(:^{1}\mathrm{S}\right)4p\right) + e^{-} \rightarrow \mathrm{Ne}^{+}\left(2p^{-2}:\,^{3}\mathrm{P}\right) + 2e^{-}\,(\mathrm{KE} = \text{about } 2\mathrm{eV}) \quad (5)$$

The final states for these peaks are likely ascribed to those with different j-components because $2p^{-2}$:^{3}P states are divided into multiplet energy levels of $^3P_0$ (0.114 eV above $^3P_2$), $^3P_1$ (0.079 eV above $^3P_2$), and $^3P_2$. Quantum defects in the relevant initial orbitals (4p) were estimated using a simple Rydberg formula, as follows:

$$T = \frac{Z_c{}^2\mathrm{Ry}}{(n-\delta)^2} \quad (6)$$

Here, T denotes the term value of the electron of interest, Z_c indicates the charge of the ion core, Ry denotes the Rydberg energy, 13.6 eV, and δ indicates the quantum defect. It is seen from table 2 that the obtained δ value of 0.64 is very close to that of a previous work [17]. The peaks near 2 eV had been reported in a previous study using the valence double photoexcitation and this peak was assigned to the initial state of $2p^{-2}(:^1S)$ 4p [20]. Panel (a) of figure 5 exhibits peaks around 2.0 eV at the perpendicular polarization significantly higher than those at the parallel polarization. The anisotropy parameters obtained are −0.65, −0.83, and −0.91 for the final states of $^3P_0$, $^3P_1$, and $^3P_2$, respectively. These β values are close to those for the similar intermediate states of ^{1}S 5p reported in the previous study [17].

Based on the study that the cascade decays through the valence double excitation provided the peak around 0.7 eV [20], peaks with low intensity located around 0.68 eV correspond to the multiplet exchange decay in the following:

$$\mathrm{Ne}^{+}\left(2p^{-2}\left(:^{1}\mathrm{S}\right)3d\right) \rightarrow \mathrm{Ne}^{2+}\left(2p^{-2}:\,^{3}\mathrm{P}\right) + e^{-}\,(\mathrm{KE} = \text{about } 0.7\mathrm{eV}) \quad (7)$$

The initial state of ^{1}S 3d is supported by the study on the threshold photoelectron spectra, in which Bolognesi *et al*

indicated the energy levels of this configuration were located at 63.16–63.27 eV [22]. The electron energy of 0.68 eV obtained here corresponds to the energy level of 63.21 eV. The quantum defects were obtained to be 0.04 or so for this excited orbital (3d). The β parameter for the cascade decay was obtained to be 0.5 in average for the four peaks. The state of ^{1}S 3d is presumed to originate from the resonant Auger decay at the first step, in which the excited 3p electron moves to the 3d orbital through a change in the azimuthal quantum number. It is interesting that the cascade decay yielding peaks of 0.68 eV in figure 5(a) is associated to the initial ^{1}S 3d state. This finding postulates that the change in the azimuthal quantum number occurs during the resonant Auger decay of the $1s^{-1}3p$ state. As mentioned in the previous section, the decay from the $1s^{-1}3p$ state into the $2p^{-2}(^1D)$ 3d state has yielded appreciably in figure 1(a) and thus, the decay into the $2p^{-2}(^1S)$ 3d state is presumed possible with a decreased rate of some factors. When the spectra measured here have been closely examined around the resonant Auger electron energy of 803.5 eV, no clear structure can be identified. However, the clear peak in figure 5(a) reflects the occurrence of the Auger decay of the change in azimuthal quantum number. The azimuthal quantum number change is considered to occur through interchannel interaction among spectator decays and participator decays, for example, the final continuum state configuration interaction among $2p^{-2}(:^1S_0)3p_{3/2}\varepsilon d_{5/2}$, $2p^{-2}(:^1S_0)3d_{5/2}\varepsilon p_{5/2}$, $2p^{-2}(:^1S_0)4s_{3/2}\varepsilon p_{5/2}$, and $2s^{-1}_{1/2}\varepsilon p_{3/2}$. These configurations correspond to the final ionic states of $2p^{-2}(:^1S_0)3p$, $2p^{-2}(:^1S_0)3d$, $2p^{-2}(:^1S_0)4s$, and $2s^{-1}$ configurations, respectively. These types of the decays are presumed to occur with very low yields in Ne, although these interchannel coupling phenomena were reported some extent in instances of Kr 3d and Xe 4d resonant photoexcitation [7, 11]. The present result shows that secondary electron emission provides a tool to clarify intermediate states in Auger decay processes. The sensitive detection of very low-energy electrons can be a useful technique for investigation of highly excited atoms and molecules.

Table 2 lists assignments and physical quantities related to the cascade Auger decays from the $1s^{-1}3p$ state; i.e., electron KEs, term values, quantum defects, and so forth. The physical quantities related to the cascade processes at the photoexcitation to the $1s^{-1}4p$ state and $1s^{-1}5p$ state are also indicated in table 2, together with corresponding values from previous studies [17, 20]. The electron KE spectra at 868.7 eV (4p excitation) and 869.3 eV (5p excitation) are shown in figures 5(b) and (c), respectively. At 4p photoexcitation, the five peaks near 0.3 eV are likely assigned to the decays from initial states of ^{1}D 5p into the final state of ^{3}P [17, 20]. The β value was estimated to be 0.21 as the average for the five peaks. The peak at 0.84 eV is presumed to originate from the decay of the ^{1}S 5p initial state into the ^{1}D final state. The decay related to the peaks near 1.3 eV is ascribed to the ^{1}D 6p initial states and the ^{3}P final state. The peak at 1.83 eV is presumed to originate from the decay of the ^{1}S 6p state into the ^{1}D state. The peaks around 2 and 4.0 eV correspond to the processes from the ^{1}S 4p state and the ^{1}S 5p initial states into the ^{3}P final state, respectively. This series of the cascade decays yields anisotropic electron emission; the β values are −0.95 for the ^{1}S 4p states and −0.97 for the ^{1}S 5p states. The quantum defect values estimated here in the instance of the 4p and 5p photoexcitations are close to those found by De Fanis *et al* [17]. The present β values also are close to those corresponding to the same decay series in the previous study [17]. At 5p photoexcitation, peaks around 1.77 eV are ascribed to the decay of the ^{1}D 7p state to the ^{3}P state. Because of the character of the shake-up effect in the excited 5p electron, peaks near 2 eV are presumed to originate from the intermediate states of ^{1}D 8p, which decay to ^{3}P states, instead of the ^{1}S 4p states.

Becker *et al* provided spectra of electron KE and assignments for the decay processes [20]. However, because only a few values for KEs were reported, energy values for peak structures have been estimated from their spectra in the present study. The corresponding term values and quantum defects have been also calculated here; these values are listed in table 2. The present values for listed physical quantities are in agreement with those by Becker *et al* [20], whereas their results include some data, which are not obtained in the present study, for decay processes coming from different excitation manners. Armen and Larkins noted the importance of cascade Auger electron emission through multiplet exchanging from valence satellite states of Ne and Ar [36]. Then, they calculated the KEs of secondly emitted electrons, as well as the decay rates through multiplet exchange transitions, using a single-configuration Hartree–Fock approximation. Their energy for the decay process (5) of Ne was 3.72 eV, which is higher than the experimental results by Becker *et al* [20] and the present study, which was around 2.08 eV. The energies for the decay from the ^{1}D 5p and the ^{1}D 6p states were 0.62 and 1.56 eV, slightly higher than the measured results, which were near 0.32 eV and near 1.30 eV, respectively.

Intensity distributions of electron signals in the present results are different from those obtained by De Fanis *et al* [17]. This finding is reasonable, as shown by the 2D maps in figures 3 and 4, bearing in mind that their photon energies were slightly higher than the present measurements. Further, the present intensity distributions are not the same as the spectra found by Becker *et al* [20], in which the photoexcitation at the lower photon energy was used and the electron energy resolution was moderate.

4. Summary

Secondary electron spectra with low KE following photoexcitation to some Rydberg orbitals have been measured in the Ne 1s photoexcitation region. At 3p excitation, a new decay channel for the resonant Auger transition and subsequent cascade electron emission has been identified using the 2D mapping technique. The electrons with approximately 0.68 eV KEs have been assigned to multiplet exchange cascade electrons from the $2p^{-2}$ (^{1}S) 3d state. This state is formed through the resonant Auger transition from the $1s^{-1}3p$ state, in which the spectator 3p electron changes its azimuthal

quantum number. Several decay channels were found to occur at the $1s^{-1}4p$ and $1s^{-1}5p$ photoexcitations, confirming the Auger cascade phenomena through previous studies using different excitation techniques. The highly sensitive detection of low-energy electrons, combined with the 2D mapping technique, proposes an efficient tool for research on the dynamical behavior of charged atoms and unstable species.

Acknowledgements:

This study was conducted with the approval of the SPring-8 Proposal Review Committee (Proposals 2008A2062 and 2013B1913). IHS expresses appreciation for support by Dr M Koike at Advanced Institute of Industrial Science and Technology during this study.

References

[1] Rubensson J E, Neeb M, Bringer A, Biermann M and Eberhardt W 1996 *Chem. Phys. Lett.* **257** 447
[2] Saito N, Kabachnik N M, Shimizu Y, Yoshida H, Ohashi H, Tamenori Y, Suzuki I H and Ueda K 2000 *J. Phys. B: At. Mol. Opt. Phys.* **33** L729
[3] Kivimäki A, Heinäsmäki S, Jurvansuu M, Alitalo S, Nõmmiste E, Aksela H and Aksela S 2001 *J. Electron Spectrosc. Relat. Phenom.* **114** 49
[4] Hentges R, Müller N, Viefhaus J, Heinzmann U and Becker U 2004 *J. Phys. B: At. Mol. Opt. Phys.* **37** L267
[5] Hergenhahn U, De Fanis A, Prümper G, Kazansky A K, Kabachnik N M and Ueda K 2005 *J. Phys. B: At. Mol. Opt. Phys.* **38** 2843
[6] Hergenhahn U, De Fanis A, Prümper G, Kazansky A K, Kabachnik N M and Ueda K 2006 *Phys. Rev.* A **73** 022709
[7] Aksela H, Kivilompolo M, Nõmmiste E and Aksela S 1997 *Phys. Rev. Lett.* **79** 4970
[8] Shimizu Y *et al* 2000 *J. Phys. B: At. Mol. Opt. Phys.* **33** L685
[9] Ueda K *et al* 2003 *Phys. Rev. Lett.* **90** 153005
[10] Pieve D, Avaldi L, Camilloni R, Coreno M, Turri G, Ruocco A, Fritzsche S, Kabachnik N M and Stefani G 2005 *J. Phys. B: At. Mol. Opt. Phys.* **38** 3619
[11] Jauhiainen J, Aksela H, Sairanen O P, Nõmmiste E and Aksela S 1996 *J. Phys. B: At. Mol. Opt. Phys.* **29** 3385
[12] Armen G B 1996 *J. Phys. B: At. Mol. Opt. Phys.* **29** 677
[13] Penent F, Sheinerman S, Andric L, Lablanquie P, Palaudoux J, Becker U, Braune M, Viefhaus J and Eland J H D 2008 *J. Phys. B: At. Mol. Opt. Phys.* **41** 045002
[14] Yoshida H *et al* 2000 *J. Phys. B: At. Mol. Opt. Phys.* **33** 4343
[15] De Fanis A, Prümper G, Hergenhahn U, Oura M, Kitajima M, Tanaka T, Tanaka H, Fritzsche S, Kabachnik N M and Ueda K 2004 *Phys. Rev.* A **70** 040702
[16] Yoshida H, Sasaki J, Kawabe Y, Senba Y, De Fanis A, Oura M, Fritzsche S, Sazhina I P, Kabachnik N M and Ueda K 2005 *J. Phys. B: At. Mol. Opt. Phys.* **38** 465
[17] De Fanis A, Prümper G, Hergenhahn U, Kukk E, Tanaka T, Kitajima M, Tanaka H, Fritzsche S, Kabachnik N M and Ueda K 2005 *J. Phys. B: At. Mol. Opt. Phys.* **38** 2229
[18] Kitajima M *et al* 2006 *J. Phys. B: At. Mol. Opt. Phys.* **39** 1299
[19] Turri G, Battera G, Avaldi L, Camilloni R, Coreno M, Ruocco A, Colle R, Simonucci S and Stefani G 2001 *J. Electron Spectrosc. Relat. Phenom.* **114/116** 199
[20] Becker U, Hemmers O, Langer B, Lee I, Menzel A, Wehlitz R and Amusia M Y 1993 *Phys. Rev.* A **47** R767
[21] NIST 2013 *NIST Atomic Spectra Database* http://physics.nist.gov/asd
[22] Bolognesi P, Avaldi L, Cooper D R, Coreno M, Camilloni R and King G C 2002 *J. Phys. B: At. Mol. Opt. Phys.* **35** 2927
[23] Ukai M, Machida S, Kameta K, Kitajima M, Kouchi N, Hatano Y and Ito K 1995 *Phys. Rev. Lett.* **74** 239
[24] Hikosaka Y, Hattori H, Hikida T and Mitsuke K 1996 *J. Chem. Phys.* **105** 6367
[25] Berrah N, Langer B, Wills A, Kull E and Bozek J D 1998 *Synchrotron Rad. News* **11** 21
[26] Sokell E, Wills A A, Wiedenhoeft M, Feng X, Rolles D and Berrah N 2005 *J. Phys. B: At. Mol. Opt. Phys.* **38** 1535
[27] Suzuki I H, Kono Y, Ikeda A, Ouchi T, Ueda K, Takahashi O, Higuchi I, Tamenori Y and Nagaoka S 2011 *J. Chem. Phys.* **134** 084312
[28] Hikosaka Y, Kaneyasu T, Shigemasa E, Tamenori Y and Kosugi N 2007 *Phys. Rev.* A **75** 042708
[29] Ohashi H, Ishiguro E, Tamenori Y, Kishimoto H, Tanaka M, Irie M, Tanaka T and Ishikawa T 2001 *Nucl. Instrum. Methods* A **467–468** 529
[30] Tamenori Y, Ohashi H, Ishiguro E and Ishikawa T 2002 *Rev. Sci. Instrum.* **73** 1588
[31] Hirono T, Kimura H, Tamenori Y, Saitoh Y, Hatano T, Tanaka T and Ishikawa T 2004 *AIP Conf. Proc.* **705** 187
[32] Schmidt V 1997 *Electron Spectrometry of Atoms using Synchrotron Radiation* (Cambridge: Cambridge University Press) chapter 6
[33] Kato M, Morishita Y, Oura M, Yamaoka H, Tamenori Y, Okada K, Matsudo T, Gejo T, Suzuki I H and Saito N 2007 *AIP Conf. Proc.* **879** 1121
[34] Siegbahn K *et al* 1969 *ESCA Applied to Free Molecules* (Amsterdam: North-Holland) pp 156–63
[35] Persson W 1971 *Phys. Scr.* **3** 133
[36] Armen G B and Larkins F P 1992 *J. Phys. B: At. Mol. Opt. Phys.* **25** 931